Ion-cross-linked Hybrid Photochromic Hydrogels with Enhanced Mechanical Properties and Shape Memory Behaviour

Shijun Long *, Fan Chen, Han Ren, Yali Hu, Yiwang Huang, Chao Chen *, Xuefeng Li *

Posted Date: 27 February 2024

doi: 10.20944/preprints202402.1563.v1

Keywords: photochromic hydrogels; ion-cross-linked hybrid hydrogels; double network; high mechanical strength; shape memory

Article

Ion-Cross-Linked Hybrid Photochromic Hydrogels with Enhanced Mechanical Properties and Shape Memory Behaviour

Shijun Long [1,2,3,*], Fan Chen [1], Han Ren [1], Yali Hu [1], Chao Chen [4,*], Yiwan Huang [1,2] and Xuefeng Li [1,2,3,*]

[1] Hubei Provincial Key Laboratory of Green Materials for Light Industry, Hubei University of Technology, Wuhan 430068, China; chenfan202301@163.com (F.C.); renhann@126.com (H.R.); hu_yali1@163.com (Y.H.); yiwanhuang@hbut.edu.cn (Y.H.)

[2] Hubei Longzhong Laboratory, Xiangyang, 441000, PR China

[3] New Materials and Green Manufacturing Talent Introduction and Innovation Demonstration Base, Hubei University of Technology, Wuhan, 430068, PR China

[4] Hubei Key Laboratory of Polymer Materials, Hubei University, 430062, Wuhan, PR China

* Correspondence: longshijun.hp@163.com (S.L.); chenchao@hubu.edu.cn (C.C.); li_xf@mail.hbut.edu.cn (X.L.)

Abstract: Shape-shifting polymers usually require not only reversible stimuli-responsive ability, but also strong mechanical properties. A novel shape-shifting photochromic hydrogel system was designed and fabricated through embedding hydrophobic spiropyran (SP) into double polymeric network (DN) by micellar copolymerization. Here, sodium alginate (Alg) and poly acrylate-co-methyl acrylate-co-spiropyran (P(SA-co-MA-co-SPMA)) were employed as the first network and the second network respectively to realize high mechanical strength. After soaked in the $CaCl_2$ solution, the carboxyl groups in the system undergo metal complexation with Ca^{2+} to enhance the hydrogel. Moreover, after the hydrogel is exposed to UV-light, the closed isomer of spiropyran in the hydrogel network can be converted into an open zwitterionic isomer MC, which is considered to interact with Ca^{2+} ions. Interestingly, Ca^{2+} and UV-light responsive programmable shape of the copolymer hydrogel can recover to its original form by immersing in pure water. Since its excellent metal ion and UV-light stimuli-responsive and mechanical properties, the hydrogel has potential applications in the field of soft actuators.

Keywords: photochromic hydrogels; ion-cross-linked hybrid hydrogels; double network; high mechanical strength; shape memory

1. Introduction

Hydrogels are soft and wet materials that exhibit a three-dimensional network with good flexibility, hydrophilicity and biocompatibility, which render them ideal as soft actuators. Therefore, stimulus-responsive hydrogels have attracted considerable attention in various fields [1] owing to their promising application prospects [2], including information recording [3], biosensors [4], actuators [5], regenerative medicine [6] and other fields [7]. Recently, the development of intelligent materials has prompted increasing interest in flexible and stretchable multi-functional intelligent hydrogels. However, conventional intelligent hydrogels typically possess a single response performance and limited mechanical properties, which greatly hinder their practical applications [8,9].

Specifically, for photoresponsive hydrogels, photochromic monomers, such as spiropyran (SP) [10–12], 4,4-bipyridine [13], azobenzene [14] and diarylethenes [15], have been introduced into hydrogels to develop optical displays. Photochromic moieties can be integrated into hydrogel structures via dynamic coordination [16], in situ co-polymerisation [17], dynamic host-guest interaction [18] and micellar co-polymerisation [19]. As an organic material with reversible photochromic property, SP undergoes a reversible intramolecular rotation between coloured and

 doi:10.20944/preprints202402.1563.v1

colourless isomers upon ultraviolet (UV) and visible light irradiation [20]. Moreover, under UV light exposure, the closed isomer of SP in the hydrogel network can be converted into open zwitterionic isomer merocyanine (MC) [21].

Nowadays, manufacturing high-strength hydrogels is not an arduous task [22,23]. Several types of high-strength hydrogels have been prepared, including double-network [24], nanocomposite [25], ion-cross-linked [26], hydrophobic interaction [27] and hybrid cross-linked hydrogels [28]. As a representative example of tough hydrogels, double-network hydrogels are composed of two mutually permeable and independent networks. When single-network hydrogels are subjected to external forces, energy dissipation within the hydrogel proceeds via a single pathway, resulting in weak mechanical properties. Conversely, owing to the synergistic effect of the two networks, the double-network hydrogels are effectively strengthened and toughened [29,30]. Among them, the hybrid cross-linked hydrogels typically consist of a singular network with multiple cross-linking points that increase the cross-linking density, which can be precisely adjusted for substantially enhanced mechanical properties [31,32]. Consequently, the hybrid cross-linked hydrogels based on ion coordination cross-linking have the advantages of a simplified preparation process and exceptional mechanical properties [33]. Benefitting from the dynamic reversible characteristics of ionic cross-links, the cross-linking strength can be controlled by pH or by introducing competitive ligands, which endows the hydrogels with reversible shape memory function [34].

Herein, a photochromic hydrogel with shape memory property and high mechanical strength was prepared by embedding acrylate derivatives of SP functional groups (SPMA) into a double-network hydrogel via the micellar co-polymerisation method. Figure 1 shows the synthetic route for the ion-cross-linked hybrid double-network photochromic hydrogel using a simple one-step method. As shown in Figure 1b, the natural polymer sodium alginate (Alg) was used as the first network and poly(acrylate-*co*-methyl acrylate-*co*-spiropyran) (P(SA-*co*-MA-*co*-SPMA)) was used as the second network. In addition, Ca^{2+} was introduced into the hydrogel network to form coordination complexation with carboxyl ($–COO^-$) groups from the two molecular chains of Alg and P(SA-*co*-MA-*co*-SPMA) to obtain high-strength ion-cross-linked hybrid photochromic hydrogels [35,36]. The ionic cross-links and covalent cross-links in the system synergistically enhance the hydrogel properties to obtain a high-strength hybrid cross-linked double-network hydrogel, which exhibits shape memory property owing to the dynamic reversible characteristics of the ionic cross-links. In addition, as shown in Figure 1c, the photochromic structure in the hydrogel network changes from the colourless closed SP state to the purple open MC zwitterionic isomer state upon UV-light irradiation. The increase in polarity leads to the interaction between amphoteric MC isomer and $–COO^-$ and Ca^{2+} on the molecular chain of the hydrogel, which further enhances its mechanical properties and extends its shape recovery time.

 doi:10.20944/preprints202402.1563.v1

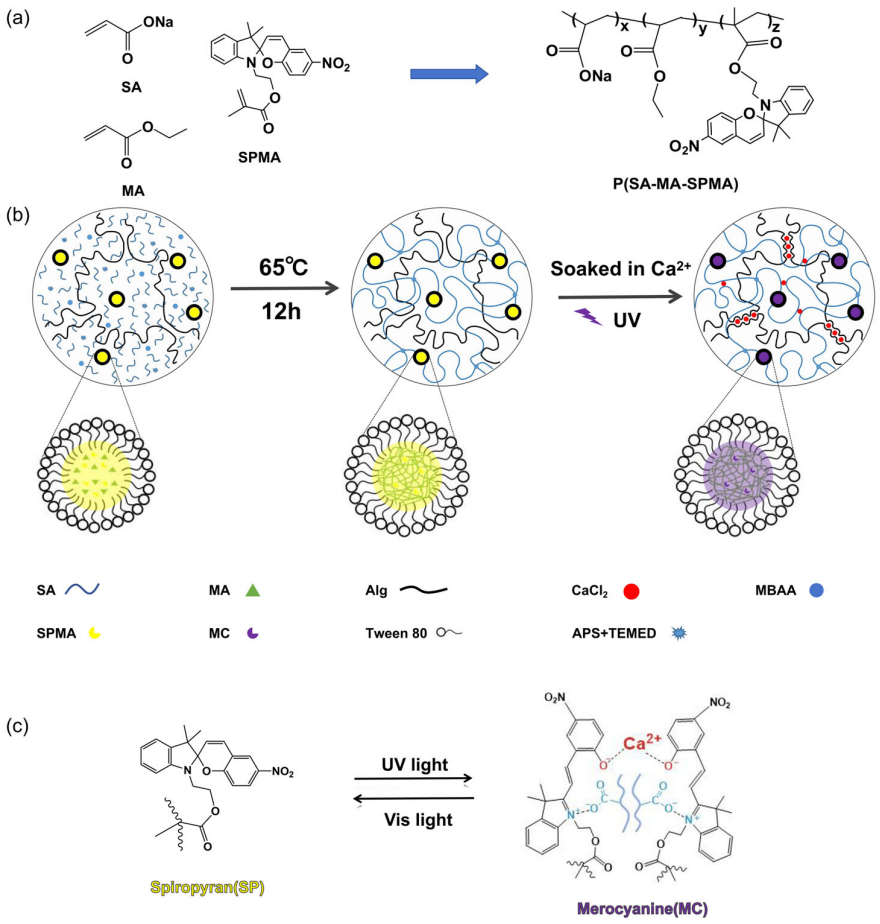

Figure 1. (a) Monomer bonding mode in the poly(sodium acrylate-*co*-methyl acrylate-*co*-spiropyran) (P(SA-*co*-MA-*co*-SPMA)) network; (b) Synthesis route for the hybrid cross-linked double-network photochromic hydrogel; (c) Under the irradiation of ultraviolet (UV) and visible (vis) light, the reversible structural transition between spiropyran (SP, closed ring) and merocyanine (MC, open ring) can trigger colour change and recovery, respectively. The more polar MC can interact and coordinate with carboxylate ions and Ca^{2+} in the polymer chain (MBAA, *N*,*N*′-methylenebis(acrylamide); APS, ammonium persulfate; TEMED, *N*′,*N*′-tetramethylethylenediamine).

2. Materials and Methods

2.1. Materials

Sodium alginate powder (Alg), sodium acrylate (SA) and methyl acrylate (MA) were purchased from Aladdin Industrial Corporation; *N*,*N*′-methylenebis(acrylamide) (MBAA), ammonium persulfate (APS), Tween 80 and anhydrous $CaCl_2$ were supplied by Sinopharm Chemical Reagent Co. Ltd. 4-Dimethylaminopyridine (DMAP), *N*,*N*′-dicyclohexyl carbinimide (DCC) and *N*′,*N*′-tetramethylethylenediamine (TEMED) were purchased from Aladdin Industrial Corporation. 1-(2-Hydroxyethyl)-3,3-dimethylindolino-6′-nitrobenzopyrylospiran (SPOH) was supplied by TCI (Shanghai) Development Co. Ltd. Deionised water was used in all experiments (18.2 Ω-cm resistivity at 25 °C).

2.2. Preparation of SPMA

The SPMA monomer was synthesised via esterification of *α*-methacrylic acid and the photochromic compound SPOH using CH_2Cl_2 as a solvent, DCC as a dehydrating agent and DMAP

 doi:10.20944/preprints202402.1563.v1

as a catalyst. Figure S1a shows a schematic of the synthesis process. The preparation process was as follows: SPOH (0.2 g), α-methacrylic acid (0.488 g), DMAP (0.07 g), DCC (1.756 g) and CH_2Cl_2 (100 mL) were added to a three-neck flask, which was stored in dark under nitrogen gas for the reaction to proceed at room temperature for 24 h. After the reaction, the mixture was extracted with CH_2Cl_2, washed successively with 10% HCl, saturated $NaHCO_3$ and deionised water. The resulting colourless liquid was separated, dried over anhydrous $MgSO_4$ and filtrated. After solvent evaporation, the product was recrystallised from hexane:benzene (1:1, v:v) and vacuum dried at 45 °C for 48 h. ^{1}H NMR (400 MHz, $CDCl_3$, TMS, ppm): δ = 8.03–7.99 (m, 2H, H_{13} and H_{14}), 7.21 (td, 1H, H_{15}), 7.10 (d, 1H, H_{11}), 6.90 (dd, 2H, H_{10} and H_{12}), 6.75 (d, 1H, H_8), 6.71 (d, 1H, H_9), 6.07 (t, 1H, H_2), 5.87 (d, 1H, H_7), 5.56 (t, 1H, H_2), 4.30 (t, 2H, H_3), 3.59–3.40 (m, 2H, H_4), 1.92 (t, 3H, H_1), 1.28 (s, 3H, H_5) and 1.17 (s, 3H, H_6) (Figure S1b). The ^{1}H NMR spectrum was recorded using a Bruker AVANCE III-400 instrument at room temperature.

2.3. Preparation of Hybrid Cross-Linked Double-Network Photochromic Hydrogels

Firstly, the photochromic monomer SPMA (0.1 mol% MA) was dissolved in the hydrophobic monomer MA (50 wt% SA) to form an oil phase, and sodium Alg powder (1.6 wt% SA), SA (2.5 mol/L) and the MBAA cross-linking agent (0.4 mol% SA) were dissolved in deionised water to form an aqueous phase. Then, under the action of the Tween 80 emulsifier (1.5 wt% water), the oil phase was uniformly dispersed in the water phase using a high-speed dispersion machine to prepare a pre-polymer solution. Finally, 0.2 mol% of REDOX initiators (APS and TEMED) was added to the pre-polymer solution to form a mixed aqueous solution, which was poured into a reaction tank (100 mm × 100 mm) composed of a pair of parallel glass plates and a polyester film separated by a hollow silicone rubber gasket with a thickness of about 1 mm. The mixture was reacted in an oven at 65 °C for 12 h and then polymerised to form Alg/P(SA-*co*-MA-*co*-SPMA) double-network photochromic hydrogel.

The resulting hydrogels were soaked in $CaCl_2$ solutions of different concentrations to introduce ionic coordination cross-linking points, affording high-strength ion-cross-linked hybrid Alg/P(SA-*co*-MA-*co*-SPMA)/Ca^{2+} photochromic hydrogels. To ensure the accuracy of the $CaCl_2$ solution concentration during immersion, three hydrogel samples (30-mm long, 5-mm wide and 1-mm thick) were immersed in 50 mL of $CaCl_2$ aqueous solution for 12 h. The corresponding samples were defined as Alg/P(SA-*co*-MA-*co*-SPMA)/$Ca^{2+}$$_{XM}$, where x is the concentration of Ca^{2+} in the impregnation solution, and Alg/P(SA-*co*-MA-*co*-SPMA)/Ca^{2+}-UV, where UV is the hydrogel irradiated with UV light. P(SA-*co*-MA-*co*-SPMA)/Ca^{2+} hydrogels were prepared using the same reagent concentration and preparation method as described above but without the sodium Alg network.

2.4. Measurements

2.4.1. Tensile Measurement

At room temperature, uniaxial tensile tests were conducted using an electronic universal tensile testing machine on rectangular hydrogel samples at a constant tensile speed of 50 mm min^{-1}. The sensor was set to 1 kN. Unless otherwise specified, three measurements were performed for each sample. The elastic modulus (E) was calculated from the slope (5%–10%) of the initial linear region of the stress–strain curve. The work of tension was determined by integrating the area under the stress–strain curve until the sample breaks. The nominal stress (σ) was calculated from the tensile force and the initial cross-sectional area of the sample as follows:

$$\sigma = F/bd \quad (1)$$

where F is the maximum load of the sample, b is the sample width and d is the sample thickness.

The original gauge length was defined as the distance between the upper and lower clamps of the sample before stretching. The gauge length at the time of fracture was defined as the distance

 doi:10.20944/preprints202402.1563.v1

between the clamps at the time of fracture after the sample is continuously stretched. The elongation at break (ε) was calculated as follows:

$$\varepsilon = (L - L_0)/L_0 \quad (2)$$

where L_0 is the original gauge length of the sample and L is the gauge length when the sample breaks.

2.4.2. Fourier Transform Infrared Spectroscopy

The hydrogel was placed in a vacuum oven at 65 °C for 12 h to dehydrate the sample. The obtained solid sample was mixed with an appropriate amount of potassium bromide powder to form a uniform powder and dried in a vacuum oven at 80 °C for 3 h. The Fourier transform infrared (FTIR) spectra were recorded on a Bruker TENSOR 27 FTIR spectrometer.

2.4.3. UV–Vis Spectroscopy

A Hitachi U-3900 UV–vis spectrophotometer was used to measure the absorbance with a scanning speed of 300 nm/min. All photochromic hydrogel samples were treated with UV light using a UV curable machine (a mercury lamp with a maximum at 365 nm and an intensity of 5.3 mW cm^{-2}, ELC-500, Electro-Lite Co.). Then, the sample was irradiated with UV light for different times and the corresponding UV–vis spectra were collected. After the sample was irradiated with UV light for 30 s, the UV–vis spectra were collected after visible light irradiation for different times using a wight light LED lamp (OPPLE, 55 W) with an intensity of 0.8 mW cm^{-2}.

2.4.4. Scanning Electron Microscopy Imaging

The cross-sectional morphology of the hydrogel samples was observed using a Hitachi SU8010 field emission scanning electron microscope (SEM). In detail, samples with small notches were frozen and brittle in liquid nitrogen, and the frozen hydrogels were placed in a freeze dryer for 48 h to dehydrate them into aerohydrogels. Then, the fractured surfaces of the samples were gold-coated using a JUC-500 magnetron sputtering device (JEOL, Tokyo, Japan) and observed with an accelerating voltage of 5 kV.

2.4.5. Water Content Measurement

The water content of the hydrogels was determined by measuring the weight change after drying in a vacuum oven. Specifically, the hydrogels were wiped to remove the water from their surface and then dried at 110 °C to obtain completely dry samples. The water content (wt%) is defined as the percentage of the weight of water in the hydrogel and the total weight of the hydrogel.

2.4.6. The Shape Recovery Rate

The Alg/P(SA-*co*-MA-*co*-SPMA) hydrogel was cut into straight strips (70-mm long, 10-mm wide and 1-mm thick) and soaked in 2.8-M Ca^{2+} solution for 4 h, which was used as a ion-cross-linked agent to fix the original shape of the Alg/P(SA-*co*-MA-*co*-SPMA)/Ca^{2+} hydrogel. The strips were put into pure water at room temperature for 120 s and the hydrogel softened owing to the blocking of ionic cross-links. The straight hydrogel strip was forms a circle and soaked in 2.8-M Ca^{2+} solution for 4 h to form the temporary shape of the hydrogel strip, which the deformation angle was θ_m. Subsequently, the hydrogel circle was immersed in pure water to initiate the shape recovery, and the deformation angle after immersing in pure water for 60 s was defined as θ_r. The shape recovery rate (R_r) was defined by the following equation:

$$R_r = \theta_r/\theta_m \times 100\% \quad (1)$$

 doi:10.20944/preprints202402.1563.v1

3. Results and Discussion

3.1. FTIR Spectroscopy

The FTIR spectroscopy was performed to analyse the chemical structures of the hydrogels, as shown in Figure 2. A comparison of the FTIR spectra of the P(SA-*co*-MA-*co*-SPMA) and Alg/P(SA-*co*-MA-*co*-SPMA) hydrogels reveals the appearance of C=O symmetric stretching vibration and C–O stretching vibration peaks of Alg at 1620 and 1094 cm^{-1}, respectively, indicating successful incorporation of Alg into the P(SA-*co*-MA-*co*-SPMA) hydrogel network [37]. The carboxyl group asymmetric stretching vibrations shifted from 1570 cm^{-1} in the spectrum of P(SA-*co*-MA-*co*-SPMA) hydrogel to 1563 cm^{-1} in the spectra of Alg/P(SA-*co*-MA-*co*-SPMA) hydrogel, which indicates the formation of hydrogen bonds between the carboxyl group and hydroxyl group. Moreover, the C–O stretching vibration peak at 1078 cm^{-1} and the C=O stretching vibration peak at 1636 cm^{-1} in the FTIR spectra of the Alg/P(SA-*co*-MA-*co*-SPMA)/Ca^{2+} hydrogel are enhanced compared with those of Alg/P(SA-*co*-MA-*co*-SPMA), whereas the –COOH stretching vibration peak at 1409 cm^{-1} is weakened. These results imply that the added Ca^{2+} ions form coordination complexes with the Alg/PSA molecular chains [38].

Finally, the –C–O– stretching vibration peak at 1428 cm^{-1} and the –C–N^{+} stretching vibration peak at 1314 cm^{-1} of the Alg/P(SA-*co*-MA-*co*-SPMA)/Ca^{2+} hydrogel are enhanced after UV exposure, which indicates the photoinduced conversion of SP to MC in the polymer [39,40]. Upon UV irradiation, the stretching vibration peak owing to tertiary C–N shifted to higher energy from 1327 to 1335 cm^{-1}, whereas the –COO^{-} stretching vibration peaks at 1562 and 1454 cm^{-1} is enhanced, which may be owing to the interaction between the zwitterionic MC structure and Ca^{2+} or –COO^{-} in the network.

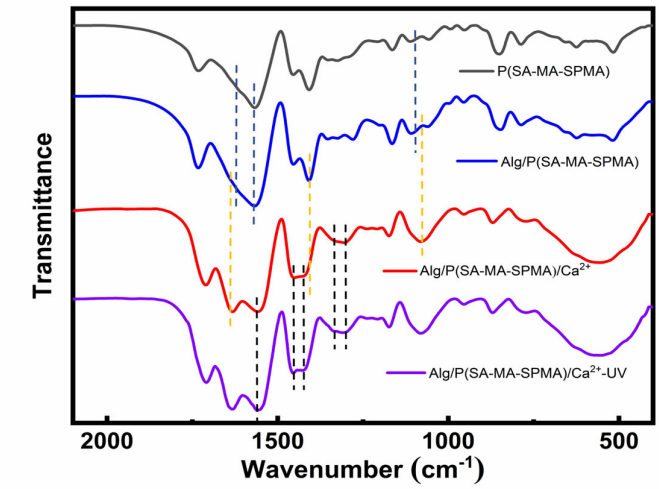

Figure 2. FTIR spectra of hydrogels, P(SA-*co*-MA-*co*-SPMA), Alg/P(SA-*co*-MA-*co*-SPMA), Alg/P(SA-*co*-MA-*co*-SPMA)/Ca^{2+} and Alg/P(SA-*co*-MA-*co*-SPMA)/Ca^{2+} after UV irradiation.

3.2. Mechanical Properties of the Hydrogels

Considering that the mechanical property is the basis of the hydrogel application, the mechanical properties of the present hydrogels were characterised by performing tensile experiments. As shown in Figure S2a, the tensile strength of the P(SA-*co*-MA-*co*-SPMA) hydrogels was less than 23 kPa with a maximum elongation at break of 220%. After the addition of Alg, the tensile strength and maximum elongation at break of the hydrogels greatly increased to 33.8 kPa and nearly 500%, respectively, because many long-chain Alg molecules entangle with the P(SA-*co*-MA-*co*-SPMA) molecular chains in the covalently cross-linked network. Simultaneously, hydrogen bonding is formed between the –COO^{-} groups in the P(SA-*co*-MA-*co*-SPMA) chains and hydroxyl

 doi:10.20944/preprints202402.1563.v1

groups in the Alg chains, obviously increasing the tightness of the whole hydrogel network. In such a network, the stress can be well dispersed when external forces are applied to the Alg/P(SA-*co*-MA-*co*-SPMA) hydrogel, thus increasing its tensile strength and elongation at break.

These results demonstrate that weak Alg/P(SA-*co*-MA-*co*-SPMA) hydrogels were converted into strong and tough hydrogels by forming Ca^{2+}–COO^- coordination complexes that act as additional cross-links to strengthen the hydrogel matrix. When the hydrogel was soaked in 2.8-M Ca^{2+} solutions, its mechanical properties reached maximum values, i.e. a tensile strength of 3.3 MPa, an elongation at break of 485% and a work of tension of 8.38 MJ m^{-3} (Figure 3b). Compared with those of the hydrogel without Ca^{2+}, the tensile strength and the work of tension increased by 97 and 98 times, respectively. This is because soaking in Ca^{2+} solutions produces not only more molecular chain entanglements but also cross-links owing to the formation of complexes between Ca^{2+} and $–COO^-$. The SEM images of the P(SA-*co*-MA-*co*-SPMA) hydrogel clearly display a multi-scale network structure containing abundant micropores with an average size of 1 μm (Figure S3b). After soaking in Ca^{2+}, no clear network structure can be observed in the SEM images of the P(SA-*co*-MA-*co*-SPMA)/$Ca^{2+}_{2.8M}$ hydrogel, which contains many micelle microspheres with an average size of 1.5 μm (Figure S3e). This is because the hydrogel network becomes dense after soaked in 2.8-M Ca^{2+}, which leads to a volume shrinkage and transparency decrease.

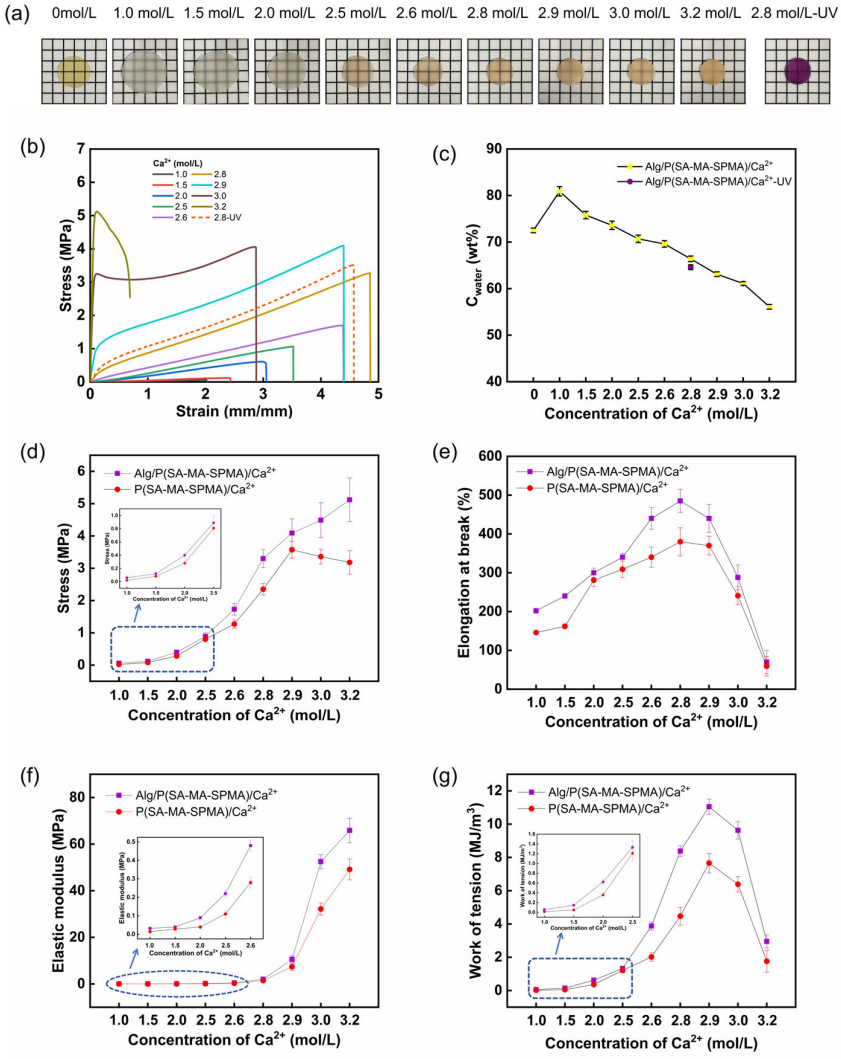

Figure 3. (a) Photos and photochromic behaviour of Alg/P(SA-*co*-MA-*co*-SPMA)/Ca^{2+} hydrogels soaked in different Ca^{2+} solutions; (b) Stress–strain curves of Alg/P(SA-*co*-MA-*co*-SPMA)/Ca^{2+}

 doi:10.20944/preprints202402.1563.v1

hydrogels soaked in different Ca^{2+} solutions; (c) Water content (C_{water}) of photochromic hydrogels before (Alg/P(SA-*co*-MA-*co*-SPMA)/Ca^{2+}) and after UV irradiation (Alg/P(SA-*co*-MA-*co*-SPMA)/Ca^{2+}-UV) soaked in different Ca^{2+} solutions. Comparison of the mechanical properties of Alg/P(SA-*co*-MA-*co*-SPMA)/Ca^{2+} double network hydrogels and P(SA-*co*-MA-*co*-SPMA)/Ca^{2+} hydrogels. (d) Tensile strength; (e) Elongation at break; (f) Elastic modulus; (g) Work of tension.

To study the effect of the Ca^{2+} concentration of the soaking solution on the mechanical properties of the Alg/P(SA-*co*-MA-*co*-SPMA)/Ca^{2+} hydrogels, the tensile properties were investigated (Figure 3b). The tensile strength of the Alg/P(SA-*co*-MA-*co*-SPMA)/Ca^{2+} hydrogel soaked in solutions with the Ca^{2+} concentrations ranging from 1.0 to 3.2 M gradually increased from 0.06 to 5.12 MPa (Figure 3d). With the continuous increase in the Ca^{2+} concentration, the concentration of the external environment solution exceeds that of the hydrogel internal environment, causing a shrinkage and decrease in the water content of the hydrogel (Figure 3c). Optical photos of the hydrogels are shown in Figure 3a. With the volume shrinkage of the hydrogel, more ionic cross-links and more entanglements are formed between the molecular chains of the hydrogel network, which are tightly clustered and have small porosity. The work of tension of the Alg/P(SA-*co*-MA-*co*-SPMA)/Ca^{2+} hydrogel also gradually increased from 0.056 to 11.05 MJ m^{-3} with increasing Ca^{2+} concentration from 1.0 to 2.9 M because the metal coordination cross-links were cleaved under external stress as, facilitating the energy dissipation (Figure 3g). The elongation at break increased first and then decreased with increasing Ca^{2+} concentration, reaching the maximum value of 485% at a Ca^{2+} concentration of 2.8 M (Figure 3e). With the increase of Ca^{2+} concentration, the elastic modulus of the hydrogel are significantly improved (Figure 3f). As shown in the images (Figure S3b), the Alg/P(SA-*co*-MA-*co*-SPMA)/$Ca^{2+}{}_{2.0M}$ hydrogel have bigger pore size than the Alg/P(SA-*co*-MA-*co*-SPMA) hydrogel. As the concentration of Ca^{2+} increases, the network structure of hydrogels shrink and such pores disappearance is visualized. Scanning electron microscopy (SEM) images of P(SA-*co*-MA-*co*-SPMA)/$Ca^{2+}{}_{2.6M}$ hydrogel clearly display many microspheres (Figure S3d). When Ca^{2+} increases, the microspheres decrease significantly in images of P(SA-*co*-MA-*co*-SPMA)/$Ca^{2+}{}_{3.0M}$ hydrogel. This is because the hydrogel network becomes denser after soaked in 3.0 M Ca^{2+}, which leads to the polymer network shrinks and tightly wraps microspheres. Upon increasing the Ca^{2+} concentration, the osmotic pressure inside and outside the hydrogel also increases, driving the hydrogel shrinkage and more Ca^{2+} ions to penetrate into the hydrogel, forming more coordination structures with the $–COO^-$ groups on the macromolecular chains and making the cross-linked network more compact, thus increasing the tensile strength and elastic modulus of the hydrogel. When the concentration of Ca^{2+} ions further increases within the range of 2.9–3.2 M, the volume of the hydrogel obviously shrinks, increasing the density of the macromolecular chains of the hydrogel. Ca^{2+} ions form excess ionic cross-links structures with the $–COO^-$ groups in the macromolecular chains, restricting the free movement of the macromolecular chain segments and in turn decreasing the elongation at break decrease to a certain extent.

After 30 s of UV irradiation, when the concentration of Ca^{2+} was 2.8 M, the tensile strength of the Alg/P(SA-*co*-MA-*co*-SPMA)/Ca^{2+} hydrogel increased by 9.4% from 3.2 to 3.5 MPa (Figure 3b), which is owing to the presence of a large number of polar zwitterionic MC structures in the network. The UV–vis spectrum of Alg/P(SA-*co*-MA-*co*-SPMA)/$Ca^{2+}{}_{2.8M}$ displayed obvious SP open-loop characteristic peaks at 538 nm, which reached saturation after 30 s of irradiation (Figure S4). At this point, simultaneously with the volume shrinkage [41], the water content of the hydrogel decreased from 66.4% to 64.6% (Figure 3c). The zwitterionic MC structures can also interact with Ca^{2+}, increasing the physical interactions in the co-polymerisation network, further enhancing the mechanical properties of the hydrogel. This result is consistent with the FTIR spectral analysis. The hydrogels also exhibited excellent photoisomerisation reversibility and fatigue resistance at room temperature. The fatigue resistance to light was investigated by subjecting the same hydrogel to 10 cycles of UV–vis irradiation (Figure S5). During the first six colouration/decolouration cycles, the intensity at λ_{max} decreased by 5%. However, during the next four cycles, the intensity at λ_{max} only decreased by another 5%. With the increasing number of cycles, the degree of reduction of the absorption intensity decreased. These results show that the metal coordination can substantially improve the mechanical

 doi:10.20944/preprints202402.1563.v1

properties of the hydrogels, which can be controllably adjusted within a certain range. The introduction of metal coordination in photochromic hydrogels can be enhanced via UV irradiation, resulting in excellent light fatigue resistance.

Next, the effect of the first network of Alg on the mechanical properties was studied. Control hydrogels without Alg exhibited similar mechanical behaviour to that of the Alg/P(SA-*co*-MA-*co*-SPMA)/Ca^{2+} double-network hydrogels. A comparison of the mechanical properties of the P(SA-*co*-MA-*co*-SPMA)/Ca^{2+} hydrogels and Alg/P(SA-*co*-MA-*co*-SPMA)/Ca^{2+} double-network hydrogels is shown in Table 1. Compared with the P(SA-*co*-MA-*co*-SPMA)/Ca^{2+} hydrogels, the Alg/P(SA-*co*-MA-*co*-SPMA)/Ca^{2+} double-network hydrogels have higher tensile strength and initial elastic modulus, indicating that the first Alg network helps improve the mechanical properties of the hydrogel. This can be attributed to Alg increasing the entanglement of the hydrogel network, which results in the formation of egg-box-like ionic interactions between Alg and Ca^{2+}, leading to more intermolecular interactions in the hydrogel networks. As a result, the ion-cross-linked hybrid double-network hydrogel has ultra-high mechanical properties that can be tuned by the ion concentration.

3.4. Shape Memory of the Hydrogels

As expected, the dynamic ionic coordination bonds endowed the hydrogels with shape memory functionalities [42]. The stability of coordination complexes is influenced by the Ca^{2+} concentration, indicating their dynamic nature. Because of the reversibility of coordination bonds of the system of P(SA-*co*-MA-*co*-SPMA) and Ca^{2+}, shape fixation and recovery of hydrogels can be realised by switching the Ca^{2+} concentration in the hydrogels. Moreover, the ion-cross-linked hydrogels usually produce reversible shape memory effect by controlling the pH value or introducing competitive ligands [34]; however, the Alg/P(SA-*co*-MA-*co*-SPMA)/$Ca^{2+}{}_{2.8M}$ hydrogel can quickly recover its shape in pure water. As shown in Figure 4a, an Alg/P(SA-*co*-MA-*co*-SPMA)/$Ca^{2+}{}_{2.8M}$ hydrogel sample was put into pure water at room temperature for 120 s and the hydrogel softened owing to the blocking of ionic cross-links. This softening indicates that the dynamic cross-links between P(SA-*co*-MA-*co*-SPMA) and Ca^{2+} were damaged, with the egg-box-like ionic interactions between Alg and Ca^{2+} and the covalent cross-links in the P(SA-*co*-MA-*co*-SPMA) network acting as permanent netpoints. After soaking the softened hydrogel in 2.8-M Ca^{2+} solution for 4 h to form and consolidate a spiral shape, the hydrogel maintained the spiral shape after removing the external force, achieving shape programming. Figure 4a shows the shape memory property of the hydrogel upon immersion in pure water and Ca^{2+} solution. The Alg/P(SA-*co*-MA-*co*-SPMA)/$Ca^{2+}{}_{2.8M}$ hydrogel can recover its original flat shape in only 120 s in pure water and in 150 s in the UV curing box (Figure 4b). The longer time required for the hydrogel to complete shape recovery under UV light is owing to the presence of abundant polar zwitterionic MC structures in the network after UV irradiation. The polarity increase may promote the interaction between the MC isomers and $–COO^-$ groups in the molecular chains of the hydrogel. Meanwhile, the zwitterionic MC structures can also interact with Ca^{2+}, increasing the physical entanglement in the co-polymerisation network, making the cross-linked network more compact. After recovering the original flat shape in pure water, the hydrogel can form a new shape by soaking in 2.8-M Ca^{2+} solution, achieving shape programming again.

 doi:10.20944/preprints202402.1563.v1

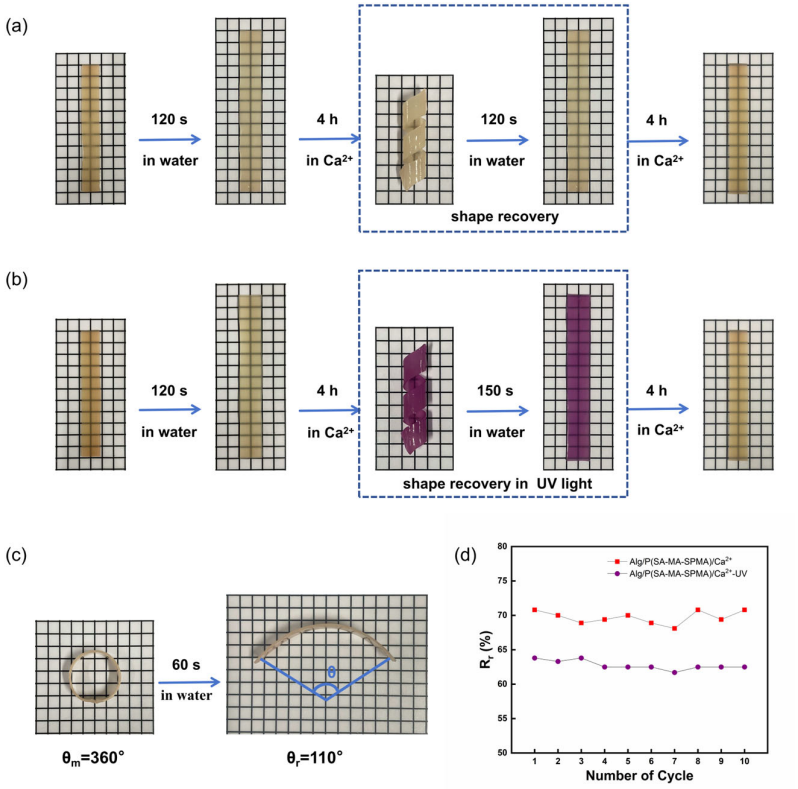

Figure 4. (a) Schematic of the shape memory behaviour of the Alg/P(SA-*co*-MA-*co*-SPMA)/$Ca^{2+}_{2.8M}$ hydrogel mediated by pure water switching; (b) Schematic of the shape memory behaviour of the Alg/P(SA-*co*-MA-*co*-SPMA)/$Ca^{2+}_{2.8M}$ hydrogel mediated by pure water switching under UV light; (c) Schematic of the shape recovery behaviour of the Alg/P(SA-*co*-MA-*co*-SPMA)/$Ca^{2+}_{2.8M}$ hydrogel forming a circle shape upon immersion in pure water for 60 s; (d) Shape recovery rate (R_r) after 10 cycles of shape fixation and relaxation of the same hydrogel sample exposed to visible light and ultraviolet light.

In practical applications of hydrogels, the reversibility of shape fixation and relaxation is very important. As shown in Figure 4c, a softened hydrogel soaked in 2.8-M Ca^{2+} solution for 4 h to consolidate the shape forms a circle with a deformation angle θ_m after shape memory. Subsequently, the hydrogel can recover its shape after immersion in pure water for 60 s, and the deformation angle after shape recovery is θ_r. The shape recovery rate (R_r) can be calculated using the ratio between θ_r and θ_m. As shown in Figures S6 and S7, the reversibility was investigated by subjecting the same hydrogel to 10 cycles of shape fixation and relaxation and separately recording the θ_m and θ_r values. As shown in Figure 4d, with the increasing number of cycles, R_r exhibits excellent repeatability, indicating the excellent reversibility of the shape fixation and relaxation of the hydrogel before and after UV irradiation.

4. Conclusions

Photochromic hydrogels with adjustable mechanical properties, photoreversible stability and shape memory properties with fast response were prepared using a simple one-pot method. The construction of an ion-cross-linked hybrid Alg/P(SA-*co*-MA-*co*-SPMA)/Ca^{2+} double network greatly improved the mechanical properties of the hydrogels. The dynamic nature of the interactions between Ca^{2+} ions and $–COO^-$ groups endows the hydrogel with shape memory behaviour in pure water and excellent reversibility of shape fixation and relaxation. Furthermore, the SP structure in the hydrogel network can be controlled via UV irradiation, which can considerably improve the tensile strength of the hydrogel and slow down the rate of shape recovery. Therefore, these ion-cross-

 doi:10.20944/preprints202402.1563.v1

linked hybrid hydrogels with multi-functionalities are attractive candidates for optical displays and various biomedical and soft artificial intelligence systems.

Supplementary Materials: The following supporting information can be downloaded at the website of this paper posted on Preprints.org, Figure S1: title; Table S1: title; Video S1: title. Figure S1: (a) The synthetic route of SPMA. (b) ^{1}H NMR spectrum of SPMA monomer (solvent $CDCl_3$, 400MHz); Figure S2: (a) Stress strain curve of P(SA-*co*-MA-*co*-SPMA) hydrogel and Alg/P(SA-*co*-MA-*co*-SPMA) hydrogel. (b) Stress strain curve of Alg/P(SA-*co*-MA-*co*-SPMA)/Ca^{2+} hydrogels soaked in solutions at different Ca^{2+} concentrations; Figure S3: SEM images for cross-sectional morphology of hydrogels (scale bar = 2 μm). (a) P(SA-*co*-MA-*co*-SPMA) hydrogel. (b) Alg/P(SA-*co*-MA-*co*-SPMA) hydrogel. (c) Alg/P(SA-*co*-MA-*co*-SPMA)/$Ca^{2+}_{2.0M}$ hydrogel. (d) Alg/P(SA-*co*-MA-*co*-SPMA)/$Ca^{2+}_{2.6M}$ hydrogel. (e) Alg/P(SA-*co*-MA-*co*-SPMA)/$Ca^{2+}_{2.8M}$ hydrogel. (f) Alg/P(SA-*co*-MA-*co*-SPMA)/$Ca^{2+}_{3.0M}$ hydrogel; Figure S4: Absorbance measurement of Alg/P(SA-*co*-MA-*co*-SPMA)/$Ca^{2+}_{2.8M}$ hydrogel after different UV irradiation times; Figure S5: Changes of A_n/A_1 during repeated coloration/discolorization cycle of Alg/P(SA-*co*-MA-*co*-SPMA)/$Ca^{2+}_{2.8M}$ hydrogel irradiated by alternative UV/vis light, where A_1 and A_n represent the intensities for the first and nth cycles at the maximum absorption wavelength; Figure S6: The photos of Alg/P(SA-*co*-MA-*co*-SPMA)/$Ca^{2+}_{2.8M}$ hydrogel conducting 10 cycles of shape fixation and shape recovery; Figure S7: The photos of Alg/P(SA-*co*-MA-*co*-SPMA)/$Ca^{2+}_{2.8M}$ hydrogel conducting 10 cycles of shape fixation and shape recovery under UV irradiation.

Author Contributions: Conceptualization, X.L. and S.L.; methodology and investigation, S.L. and F.C.; formal analysis, F.C. and S.L.; Scanning electron microscopy imaging measurements, Y.H.; tensile measurements, Y.H. and H.R.; writing—original draft preparation, F.C.; writing—review and editing, S.L. and C.C.; discussion of experiments, C.C., X.L. and S.L. All authors have read and agreed to the published version of the manuscript.

Funding: This research was supported by the National Natural Science Foundation of China (Contract no. 52073083 and 51603065).

Institutional Review Board Statement: Not applicable.

Data Availability Statement: Not applicable.

Acknowledgments: Not applicable.

Conflicts of Interest: The authors declare no conflict of interest.

References

1. Trung, T.; Lee, N. Recent progress on stretchable electronic devices with intrinsically stretchable components. *Adv. Mater.* **2017**, 29, 1603167.
2. Dong, M.; Jiao, D.; Zheng, Q.; Wu, Z. Recent progress in fabrications and applications of functional hydrogel films. *J. Polym Sci.* **2023**, 61, 1026-1039.
3. Kim, J.; Choi, S.; Lee, H.; Kwon, S. Magnetochromatic microactuators for a micropixellated color-changing surface. *Adv. Mater.* **2013**, 25, 1415-1419.
4. Zang, Y.; Zhang, F.; Di, C.; Zhu, D. Advances of flexible pressure sensors toward artificial intelligence and health care applications. *Mater. Horiz.* **2015**, 2, 140-156.
5. Chen, Z.; Liu, J.; Chen, Y.; Zheng, X.; Liu, H.; Li, H. Multiple-stimuli-responsive and cellulose conductive ionic hydrogel for smart wearable devices and thermal actuators. *ACS Appl. Mater. Interfaces* **2021**, 13, 1353-1366.
6. Chaudhuri, O.; Gu, L.; Klumpers, D.; Darnell, M.; Bencherif, S.; Weaver, J.; Huebsch, N.; Lee, H.; Lippens, E.; Duda, G.; Mooney D. Hydrogels with tunable stress relaxation regulate stem cell fate and activity. *Nat. Mater.* **2016**, 15, 326-334.
7. Zhang, Y.; Khademhosseini, A. Advances in Engineering Hydrogels. *Science* **2017**, 356, eaaf3627.
8. Sun, Y.; Le, X.; Zhou, S.; Chen, T. Recent progress in smart polymeric gel-based information storage for anti-counterfeiting. *Adv. Mater.* **2022**, 34, e2201262.
9. Wu, S.; Shi, H.; Lu, W.; Wei, S.; Shang, H.; Liu, H.; Si, M.; Le, X.; Yin, G.; Theato, P.; Chen, T. Aggregation-induced emissive carbon dots gels for octopus-inspired shape/color synergistically adjustable actuators. *Angew. Chem. Int. Ed.* **2021**, 60, 21890-21898.
10. Chen, H.; Yang, F.; Chen, Q.; Zheng, J. A novel design of multi-mechanoresponsive and mechanically strong hydrogels. *Adv. Mater.* **2017**, 29, 1606900.
11. Xiao, X.; Yang, G.; Chen, A.; Zheng, Z.; Zhang, C.; Zhang, Y.; Liao, L. Multi-responsive chromatic hydrogel exhibiting reversible shape deformations. *Dyes Pigm.* **2022**, 204, 110364.
12. Long, S.; Huang, J. Xiong, J.; Liu, C.; Chen, F.; Shen, J.; Huang, Y.; Li, X. Designing Multistimuli-Responsive Anisotropic Bilayer Hydrogel Actuators by Integrating LCST Phase Transition and Photochromic Isomerization. *Polymers* **2023**, 15, 786.

 doi:10.20944/preprints202402.1563.v1

13. Zhang, P.; Zhu, F.; Wang, F.; Wang, J.; Dong, R.; Zhuang, X.; Schmidt, O.; Feng, X. Stimulus-responsive micro-supercapacitors with ultrahigh energy density and reversible electrochromic window. *Adv. Mater.* **2017**, 29, 1604491.
14. Dai, L.; Lu, J.; Kong, F.; Liu, K.; Wei, H.; Si, C. Reversible photo-controlled release of bovine serum albumin by azobenzene-containing cellulose nanofibrils-based hydrogel. *Adv. Compos. Hybrid Mater.* **2019**, 2, 462-470.
15. Boelke J, Hecht S. Designing molecular photoswitches for soft materials applications. *Adv. Opt. Mater.* **2019**, 7, 1900404.
16. Weng, G.; Thanneeru, S.; He, J. Dynamic coordination of Eu-iminodiacetate to control fluorochromic response of polymer hydrogels to multistimuli. *Adv. Mater.* **2018**, 30, 1706526.
17. Zhang, X.; Wang, Y.; Sun, S.; Hou, L.; Wu, P.; Wu, Z.; Zheng, Q. A tough and stiff hydrogel with tunable water content and mechanical properties based on the synergistic effect of hydrogen bonding and hydrophobic interaction. *Macromolecules* **2018**, 51, 8136-8146.
18. Wang, H.; Zhu, C.; Zeng, H.; Ji, X.; Xie, T.; Yan, X.; Wu, Z.; Huang, F. Reversible ion-conducting switch in a novel single-ion supramolecular hydrogel enabled by photoresponsive host-guest molecular recognition. *Adv. Mater.* **2019**, 31, 1807328.
19. Chen, H.; Yang, F.; Chen, Q.; Zheng, J. A novel design of multi-mechanoresponsive and mechanically strong hydrogels. *Adv. Mater.* **2017**, 29, 1606900.
20. Meng, X.; Qi, G.; Zhang, C.; Wang, K.; Zou, B.; Ma, Y. Visible mechanochromic responses of spiropyrans in crystals via pressure-induced isomerization. *Chem. Commun.* **2015**, 51, 9320-9323.
21. Klajn, R. Spiropyran-based dynamic materials. *Chem. Soc. Rev.* **2014**, 45, 148-184.
22. Gu, H.; Wang, G.; Cao, X. Thermoresponsive nanocomposite hydrogels with high mechanical strength and toughness based on a dual crosslinking strategy. *J. Appl. Polym. Sci.* **2021**, 138, 51509.
23. Mu, Q.; Cui, K.; Wang, Z.; Matsuda, T.; Cui, W.; Kato, H.; Namiki, S.; Yamazaki, T.; Frauenlob, M.; Nonoyama, T.; Tsuda, T.; Tanaka, S.; Nakajima, T.; Gong, J. Force-triggered rapid microstructure growth on hydrogel surface for on-demand functions. *Nat. Commun.* **2022**, 13, 6213-6223.
24. Meng, X.; Qiao, Y.; Do, C.; Bras, W.; He, C.; Ke, Y.; Russell, T.; Qiu, D. Hysteresis-free nanoparticle-reinforced hydrogels. *Adv. Mater.* **2022**, 34, 2108243.
25. Li, X.; Xu, D.; Wang, H.; Gong, C.; Li, H.; Huang, Y.; Long, S.; Li, D. Programmed transformations of strong polyvinyl alcohol/sodium alginate hydrogels via ionic crosslink lithography. *Macromol. Rapid Commun.* **2020**, 41, 2000127.
26. Huang, G.; Tang, Z.; Peng, S.; Zhang, P.; Sun, T.; Wei, W.; Zeng, L.; Guo, H.; Guo, H.; Meng, G. Modification of hydrophobic hydrogels into a strongly adhesive and tough hydrogel by electrostatic interaction. *Macromolecules* **2022**, 55, 156-165.
27. Jiang, Z.; Song, P. Strong and fast hydrogel actuators. *Science* **2022**, 376, 245.
28. Yang, Y.; Shen, S.; Fan, D. A physicochemical double cross-linked multifunctional hydrogel for dynamic burn wound healing: shape adaptability, injectable self-healing property and enhanced adhesion. *Biomaterials* **2021**, 276, 120838.
29. Chen, Q.; Chen, H.; Zhu, L.; Zheng, J. Fundamentals of double network hydrogels. *J. Mater. Chem. B* **2015**, 3, 3654-3676.
30. Li, H.; Wang, H.; Zhang, D.; Xu, Z.; Liu, W. A highly tough and stiff supramolecular polymer double network hydrogel. *Polymer* **2018**, 153, 193-200.
31. Yu, H.; Zheng, S.; Fang, L.; Ying, Z.; Du, M.; Wang, J.; Ren, K.; Wu, Z.; Zheng, Q. Reversibly transforming a highly swollen polyelectrolyte hydrogel to an extremely tough one and its application as a tubular grasper. *Adv. Mater.* **2020**, 32, 2005171.
32. Zheng, S.; Ding, H.; Qian, J.; Yin, J.; Wu, Z.; Song, Y.; Zheng, Q. Metal-coordination complexes mediated physical hydrogels with high toughness, stick-slip tearing behavior, and good processability. *Macromolecules* **2016**, 49, 9637-9646.
33. Yang, C.; Wang, M.; Haider, H.; Yang, J.; Sun, J.; Chen, Y.; Zhou, J.; Suo, Z. Strengthening alginate/polyacrylamide hydrogels using various multivalent cations. *ACS Appl. Mater. Interfaces* **2013**, 5, 10418-10422.
34. Yasin, A.; Li, H.;, Zhao, L.; Rehman, S.;, Siddiq, M.; Yang, H. A shape memory hydrogel induced by the interactions between metal ions and phosphate. *Soft Matter* **2014**, 10, 972-977.
35. Fang, Y.; Al-Assaf, S.; Phillips, G.; Nishinari, K.; Funami, T.; Williams, P.; Li, L. Multiple steps and critical behaviors of the binding of calcium to alginate. *J. Phys. Chem. B* **2007**, 111, 2456-2462.
36. Li, X.; Zhao, Y.; Li, D.; Zhang, G.; Long, S.; Wang, H. Hybrid dual crosslinked polyacrylic acid hydrogels with ultrahigh mechanical strength, toughness and self-healing properties via soaking salt solution. *Polymer* **2017**, 121, 55-63.
37. Wu, X.; Deng, X.; Song, Y.; Zhang, Z.; Su, H.; Han, Y.; Shen, Y.; Liu, S.; Sun, K.; Yao, H.; Guan, S. Polyacrylamide/sodium alginate photochromic hydrogels with enhanced toughness and fast response for optical display and rewritable information record. *Dyes Pigm.* **2023**, 210, 111009.

 doi:10.20944/preprints202402.1563.v1

38. Long, S.; Ye, Z.; Jin, Y.; Huang, J.; Huang, Y.; Liao, Y.; Li, X. High-performance photochromic hydrogels for rewritable information record. *Macromol. Rapid Commun* **2021**, 42, 2000701.
39. Fries, K.; Driskell, J.; Samanta, S.; Locklin, J. Spectroscopic analysis of metal ion binding in spiropyran containing copolymer thin films. *Anal. Chem.* **2010**, 82, 3306-3314.
40. Fries, K.; Sheppard, G.; Bilbrey, J.; Locklin, J. Tuning chelating groups and comonomers in spiropyran-containing copolymer thin films for color-specific metal ion binding. *Polym. Chem* **2014**, 5, 2094-2102.
41. Li, C.; Iscen, A.; Palmer, L.; Schatz, G.; Stupp, S. Light-driven expansion of spiropyran hydrogels. *J. Am. Chem. Soc.* **2020**, 142, 8447-8453.
42. Shang, J.; Le, X.; Zhang, J.; Chen, T.; Theato, P. Trends in polymeric shape memory hydrogels and hydrogel actuators. *Polym. Chem.* **2019**, 10, 1036-1055.